AIRCRAFT COLLISION

Final report

Saghir Ilias, Elkadiri Salaheddine

CONTENTS

1 INTRODUCTION

In order to avoid conflicts between aircraft, aeronautical regulations provide minimum separation standards to be observed between airliners. At take-off and landing airplanes should be at least two minutes apart. And to avoid any risk of collision while cruising, airplanes operating above 5,000 m must be at least 9 km (5 nmi) horizontally and at least 300 m (1,000 ft) vertically apart.

In this project, we elaborate a probabilistic study of conflicts between planes in the medium term (20 min). A conflict becomes imminent when the prescribed separation distance between two planes is less than a given threshold. In the medium term, the various sources of uncertainty affecting the movement of the aircraft generally cause deviations from the nominal flight path, which cannot be overlooked when detecting conflicts. Calculating the probability of conflicts between aircraft trajectories is generally a delicate task as they are difficult to model, but also because their rarity prevents an exact estimate. In our work, we rely on the Erzberger-Paielli model for the generation of trajectories over durations of 20 minutes. This model involves the different deviations resulting from meteorological circumstances and other uncertainties. Obviously, the more complex the model, and the fewer conflicts, the more costly the generation of simulations in terms of computation and time. Given this constraint, we are examining important sampling solutions to accelerate the convergence of results. These solutions are inspired by rare event simulation methods.

To calculate the probabilities of conflict we used the following methods:

- **Naive Monte Carlo**: Estimating probabilities as little as 10^{-5} through simple simulations.
- **Importance sampling with change of probability**: It is a variance reduction method, which consists in calculating a Monte Carlo estimator from the simulation of observations under a different law which makes it possible to observe their realization more frequently. In our case, a change in mean (therefore nominal trajectories) or variance (uncertainty on the trajectories) acts on the frequency of collisions. Then, to adapt our change of mean, we used an adaptive optimal mean algorithm for multi-dimensional Gaussian probability changes "Lelong and Jourdain algorithm".
- **Monte-Carlo Markov Chain Methods**: The Monte Carlo Markov Chain (MCMC) method includes a class of algorithms for sampling from a probability distribution. By constructing a Markov chain that has the desired distribution as an equilibrium distribution, one can obtain a sample of the desired distribution by recording the states of the chain. The more steps included, the more closely the sample distribution matches the desired actual distribution

During this study, we mobilize and compare the tools cited in order to calculate the probability of conflict as a first step. We thus observe the effect of the flight plan (in particular the

distance between planes) on the latter. Next, we are interested in the conditional distribution of conflict time. Finally, we visualize the spacial distribution of collisions.

2
MODEL

Our study is based on a conflict probability estimation model suggested in the work of Russel A. Paielli and Heinz Erzberger (1997): "Conflict probability estimation for free flight" In this model, the aircraft's movement is considered plane, and passes through waypoints at regular intervals (20 minutes) during which the nominal trajectory is assumed to be straight. Between two waypoints, the position of an airplane is given by its coordinates in a frame centered on the first waypoint, consisting of two axes a and c : one being parallel to the direction of flight (*along-track* component) and the other perpendicular (*cross-track* component).

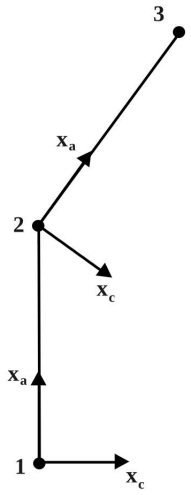

Figure 1: Example of flight plan with 3 waypoints

We limit ourselves to the study of a trajectory located between two waypoints, simulating 20 minutes of flight time. Thus, reference frame will be fixed by the initial conditions (positions and angles).

Weather hazards (such as wind), piloting disturbances, and measurement errors cause planes to follow different trajectories from the ideal flight plans above. These deviations will therefore be modeled by Gaussian perturbations of the coordinates *along-track* and *cross-track*. So, if $x_t = (x_{a,t}, x_{c,t})$ is the position of the plane over time in a local coordinate system centered on the previous waypoint, we have:

$$x_{a,t} = vt + M_{a,t} \text{ and } x_{c,t} = M_{c,t}$$

where $M_{a,t}$ and $M_{c,t}$ are centered continuous Gaussian processes with the covariance matrix being given by (for $t < s$):

$$\mathbb{C}\text{ov}(M_{a,t}, M_{a,s}) = r_a^2 t^2$$
$$\mathbb{C}\text{ov}(M_{c,t}, M_{c,s}) = \sigma_c^2(1 - e^{-2\frac{r_c}{\sigma_c}vt})e^{-\frac{r_c}{\sigma_c}v(s-t)}$$

For civil turbine aircraft, we have $r_a = 0.25$ nmi/min, $r_c = 1/57$ and $\sigma_c = 1$ nmi in the usual units.

Interpretation :

- *along-track* component : With time, the along-track coordinate is less and less certain because of the accumulation of navigation hazards, the disturbance is interpreted as an uncertainty about the speed.

- *cross-track* component : On the cross-track coordinate, the phenomenon is different and the variance of the uncertainty stabilizes when t is large. This is interpreted as follows: along the along-track component, the pilot and the on-board instruments seek to correct the deviations from the ideal trajectory inducing a return to 0 phenomenon.

For simulation purposes, we cannot consider trajectories that are continuous in time but only sampled at regular intervals, of one minute in our case. We will say that two planes are in conflict if the distance between them becomes less than a minimum threshold of 0.1 nmi at some point in their trajectories.

3 CONFLICT PROBABILITY : PARALLEL TRAJECTORIES

3.1 Simulation

Initially, we will be interested in a portion of trajectory between two waypoints, sampled by intervals of one minute. We will consider two planes with parallel trajectories and neglect the *along-track* perturbation (r_a =0). For each of the planes, the coordinates $(x_{c,t})_{1\leq t\leq 20}$ are given by a random 20 dimensional Gaussian vector whose covariance matrix has been described before, whose mean depends on the nominal distance between the two flight plans. Using the numpy library for Python, we generate simulations of those trajectories, which we then represent using the matplotlib graphics library.

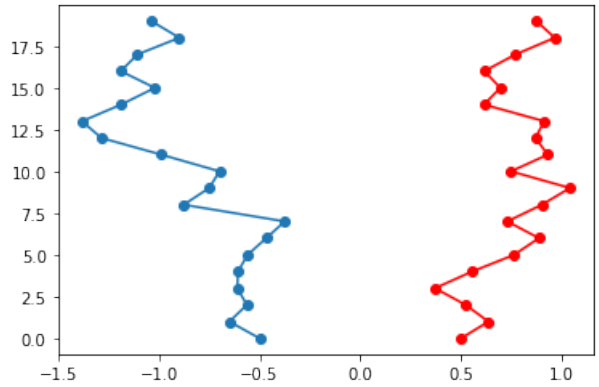

Figure 2: Simulation of two plane trajectories 1 nmi apart

3.2 First estimate

We now seek to estimate, for different flight plans, the probability of conflict. At first, we consider parallel trajectories and try to approach the probability as a function of the nominal distance between the planes d.

3.2.1 • Naive Monte-Carlo

Simulating two trajectories amounts to simulating a couple $Z = (X, Y)$ of independent Gaussian random vectors. The probability of conflict can be seen as the expected value, under the law defined by the model (covariance matrix and distance between trajectories) of a function of the pair of variables $f(Z) = 1$ if $\min_{1 \leq t \leq 20} |X_t - Y_t| < 0.1$ and 0 otherwise.

$$\mathbb{P}(A) \approx \frac{1}{N} \sum_{i=1}^{N} f(Z^{(i)})$$

We then simulate, for different values of the distance d, a large sample of pairs of trajectories ($N = 100{,}000$). We first start with small values of d which we then increase.

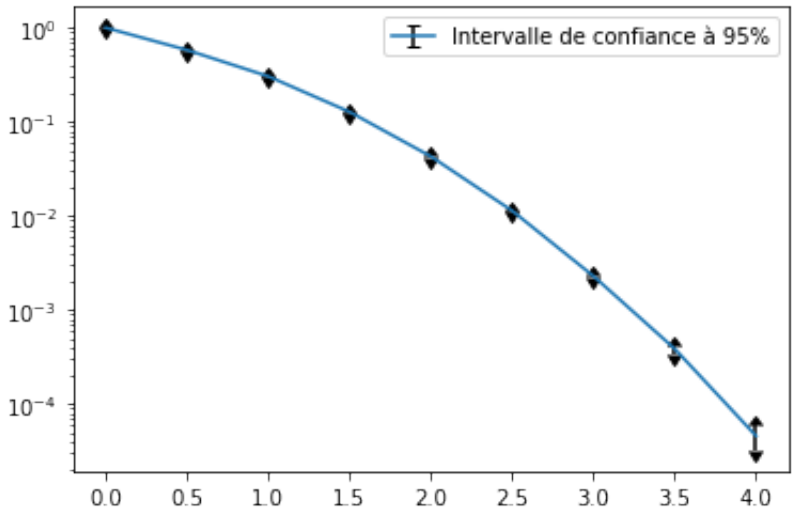

Figure 3: Probability of collision for different values of d, with 95% confidence intervals.

As we would expect, the probability decreases rapidly with distance. We note that for $d = 4$, the probability of conflict is already of the order of 10^{-5} and falls within the field of rare events. For $d = 5$, the estimator is no longer efficient.

3.2.2 • Importance sampling : mean shift

The rarity of the events that we study limits the performance of the classic Monte-Carlo estimator. We therefore use an importance sampling method based on a mean shift :

$$\mathbb{P}(A) = \mathbb{E}_{\mathbb{P}}(1_A) = \mathbb{E}_{\mathbb{Q}}(1_A \frac{d\mathbb{P}}{d\mathbb{Q}})$$

Under $\mathbb{P}$, X and Y are respectively centered on $\mu = (d/2, ..., d/2)^T$ and $-\mu = (-d/2, ..., -d/2)^T$ and $Z = (X, Y)$ is of density :

$$g(Z) = \frac{1}{(2\pi)^n det(C)} e^{-\frac{1}{2}((X-\mu)^T C^{-1}(X-\mu)+(Y+\mu)^T C^{-1}(Y+\mu))}$$

Under $\mathbb{Q}$, X and Y are respectively centered on $\mu^* = (d^*/2, ..., d^*/2)^T$ and $-\mu^* = (-d^*/2, ..., -d^*/2)^T$ and $Z = (X, Y)$ possesses the density :

$$g^*(Z) = \frac{1}{(2\pi)^n det(C)} e^{-\frac{1}{2}((X-\mu^*)^T C^{-1}(X-\mu^*)+(Y+\mu^*)^T C^{-1}(Y+\mu^*))}$$

Thus, we have for N large enough : $\mathbb{P}(A) \approx \frac{1}{N} \sum_{i=1}^{N} f(Z^{(i)}) \frac{g(Z^{(i)})}{g^*(Z^{(i)})}$ where the $Z^{(i)}$ are simulated under $\mathbb{Q}$

Indeed, the more the trajectories are distant, the lower the probability. Reducing the distance allows to observe the realization of the event more often , and a good choice of the mean shift for the Gaussian vectors provides an estimator with a smaller variance. At d fixed, the parameter d^* which minimizes the variance of the estimator is given by: $d^*_{min} = argmin\ \mathbb{E}_{d^*}[(f(Z^{(i)})\frac{g(Z^{(i)})}{g^*(Z^{(i)})})^2]$ whom we approximate through Monte-Carlo simulations of this quantity for a sample of values of d^*. However, we had difficulties implementing this method effectively, for two main reasons :

- First, the nature of the chosen mean shift, operating in the same way on all the coordinates of the vector, is not the most relevant in our case, which leads to too large a variance and sensitivity to the alpha parameter, as we will see in more detail later.
- The second limitation is mainly practical and is due to the way we implement the change of mean, in particular the choice to work with non-standard Gaussian vectors. This results in more complicated likelihood ratios to calculate and gives rise to a lot of potential code errors.

3.2.3 • Monte-Carlo with variance shift

Another way to act on the frequency of collisions is to increase the uncertainty on the trajectories, we tried to implement this in two different ways:

1. Global change :

The idea here is to multiply the covariance matrix of one of the Gaussian vectors (X for example) by a well chosen coefficient $\alpha > 1$, this has the effect of increasing the variance on the coordinates of the trajectory and therefore the uncertainty on them, and thus increase the probability of conflict. The change is as follows:
Under $\mathbb{P}$, X and Y are respectively centered on $\mu = (d/2, ..., d/2)^T$ and $-\mu = (-d/2, ..., -d/2)^T$ and the density of $Z = (X, Y)$ is given by :

$$g(Z) = \frac{1}{(2\pi)^n det(C)} e^{-\frac{1}{2}((X-\mu)^T C^{-1}(X-\mu)+(Y+\mu)^T C^{-1}(Y+\mu))}$$

Under $\mathbb{Q}$, X and Y are respectively centered on $\mu = (d/2, ..., d/2)^T$ and $-\mu = (-d/2, ..., -d/2)^T$ and and the density of $Z = (X, Y)$ is given by :

$$g^*(Z) = \frac{1}{(2\pi)^n \alpha^{\frac{n}{2}} det(C)} e^{-\frac{1}{2}((X-\mu)^T \frac{1}{\alpha} C^{-1}(X-\mu)+(Y+\mu)^T C^{-1}(Y+\mu))}$$

Once again, we have for N large enough : $\mathbb{P}(A) \approx \frac{1}{N} \sum_{i=1}^{N} f(Z^{(i)}) \frac{g(Z^{(i)})}{g^*(Z^{(i)})}$ where the $Z^{(i)}$ are simulated under $\mathbb{Q}$

Then, it's mostly about choosing the right parameter α, we can approach the optimal parameter by Monte-Carlo estimates of the variance for sampled values for α, for example, for $d = 3.5$, and $N = 100{,}000$ simulations, we have the following curve :

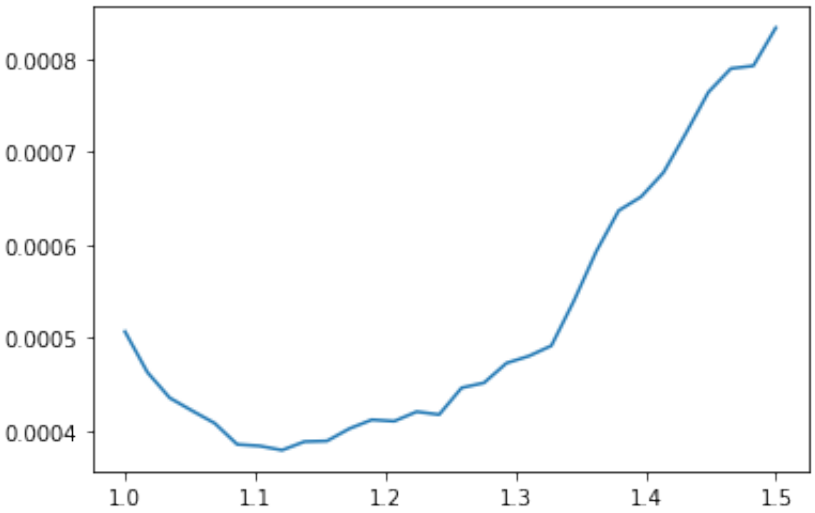

Figure 4: Empirical variance for different values of alpha

We notice that $\alpha \approx 1,1$ is a good parameter choice. When compared with the regular Monte-Carlo method, this estimator is much more efficient :

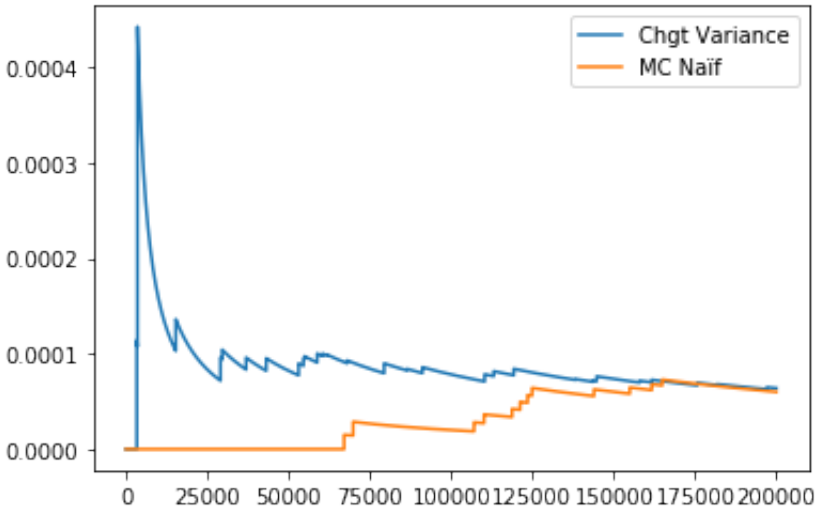

Figure 5: Naive MC vs. Variance shift

We do this for different values of d in order to obtain acceptable confidence intervals for the probabilities of conflict :

Distance	4	4,5	5	5,5	6
α	1,4	2,25	2,8	3,4	4
CI 95%	$[6, 7.10^{-5}, 7, 8.10^{-5}]$	$[4, 8.10^{-6}, 8.10^{-6}]$	$[2, 1.10^{-7}, 6, 7.10^{-7}]$	$\leq 1, 3.10^{-7}$	$[8, 1.10^{-11}, 7, 1.10^{-10}]$

Conclusion :

Our first approach based on importance sampling was driven by early hunches about what might influence collision frequency. But in view of the results obtained, our understanding, as well as our methods, could be further improved.

3.3 Refined study

3.3.1 • Some remarks and adjustments :

Before continuing, it is necessary to clarify some details related to the implementation of the model:

- First of all, so far the speed of the planes has been set at $v = 1$ nmi/min. The usual airliner speed being around 8 nmi/min, this parameter had to be corrected later for a more realistic model. Therefore, some values calculated in the following differ from those calculated previously. Indeed, at d fixed, for $r_a = 0$ we observe an increase in the probability of conflict with the speed.

- Secondly, we have previously mentioned the importance of a simple and numerically efficient implementation in the functioning of the methods and the determination of the optimal parameters. For that, we chose to lighten our codes by adopting, for example for the case of parallel trajectories, the modeling by only one vector representing the difference between the coordinates textit cross-track. This vector, centered with covariance $2C$ is obtained by the transform of a standard Gaussian vector: $\sqrt{2}C^{\frac{1}{2}}X + 2\mu$ where $X \sim \mathcal{N}(0, I_{20})$, the latter will be subject to the law change, and therefore the likelihood ratio is much easier to express and compute for large samples.

- Finally, we also saw that the law changes operating in the same way on all coordinates were not effective. Indeed, the model does not have the same behavior at all times, certain times of conflicts are more likely than others, and this should be taken into account in the importance sampling in order not to cause too large a variance. of the estimator.

3.3.2 • Lelong Jourdain algorithm :

We have previously expressed a difficulty in the implementation of the mean shift. After reviewing our code, we were able to implement the method and observe its performance. However, determining the change vector θ remains critical. Until then, we were looking for the optimal parameter among a restricted set $Vect\ (1, ..., 1)^T\}$, but this choice could be improved. For

this, we used an adaptive optimal mean algorithm for multidimensional Gaussian probability changes (Lelong and Jourdain algorithm). This algorithm exploits the relation:

$$\mathbb{E}[f(X)] = \mathbb{E}\left[f(X+\theta)\, e^{-\langle\theta,X\rangle - \|\theta\|^2/2}\right],$$

Where $X \sim \mathcal{N}(0, I)$, in our case f is defined by $f(\mathbf{x}) = \mathbf{1}_{\min(|\sqrt{2}C^{\frac{1}{2}}\mathbf{x}+2\mu|)<0.1}$. We must determine the parameter θ_* that minimizes the variance and thus the quantity :

$$\nu(\theta) = \mathbb{E}\left[f^2(X)e^{-\langle\theta,X\rangle+\|\theta\|^2/2}\right]$$

This parameter is approximated using a noisy version of Newton's Method: for a fixed n, $\theta_\star$ is approximated with θ_n which is defined as the limit when k tends to infinity, of the sequence $\{t_k, k \geq 0\}$ which satisfies

$$t_{k+1} = t_k - (H_n(t_k))^{-1}\, G_n(t_k)$$

where $H_n(t), G_n(t)$ are the Monte Carlo approximations of the hessian $H(t)$ and gradient $G(t)$ calculated from the same n independent observations $X_1, \cdots, X_n$ of a $N_{20}(0, I_{20})$ distribution:

$$G_n(\theta) = \frac{1}{n}\sum_{k=1}^{n} f^2(X_k)(\theta - X_k)e^{-\langle\theta,X_k\rangle+\|\theta\|^2/2},$$

$$H_n(\theta) = \frac{1}{n}\sum_{k=1}^{n} f^2(X_k)\left(I_d + (\theta - X_k)(\theta - X_k)'\right) e^{-\langle\theta,X_k\rangle+\|\theta\|^2/2}.$$

In practice, t_0 is initialized to 0, and in order to obtain reasonable execution times, we set the sample size to $n = 10,000$ and the maximum number of iterations of Newton's algorithm at $m = 100$. This allows us to observe the convergence for small distances:

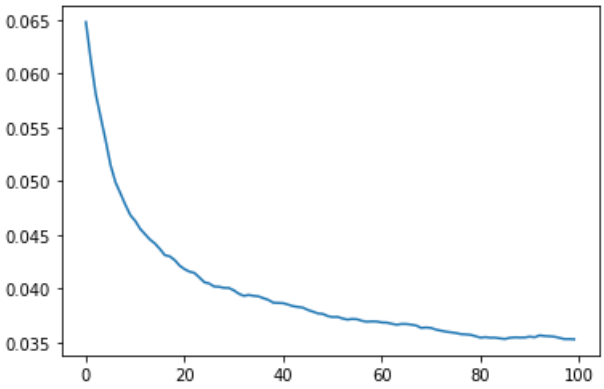

Figure 6: $\nu(t_k)$ throughout iterations of Newton's algorithm ($d = 3$, $v = 8$, $r_a = 0$)

However, as the probability of conflict decreases, the variance, gradient, and Hessian estimates become less reliable, which prevents convergence of Newton's noisy algorithm. Thus, we encountered a difficulty in generalizing this method for greater distances, but these results were not useless to us. Indeed, we noticed that the algorithm returned vectors θ_n increasing in absolute value, so that the optimal change of mean seemed to act more on the last part of the trajectory, which inspired us later.

3.3.3 • Improved mean shift :

In this part, we use the probability shift:

$$\mathbb{E}[f(X)] = \mathbb{E}\left[f(X+\theta)\, e^{-\langle\theta, X\rangle - \|\theta\|^2/2}\right],$$

This time, we are looking for the optimal mean θ_* in the form $\theta = \lambda \mathbf{u}$, where $\mathbf{u}$ is a "kernel" vector of change, with components in $[0, 1]$ that are increasing ($u_i \leq u_{i+1}$) and $\lambda \in \mathbb{R}$ that we choose in order to minimize $\nu(\theta)$. We have considered several paces for $\mathbf{u}$: linear, exponential, quadratic, logarithmic growth...

When $r_a = 0$:

When the uncertainty on the *along-track* component is neglected, we have the best results for the following two allures:

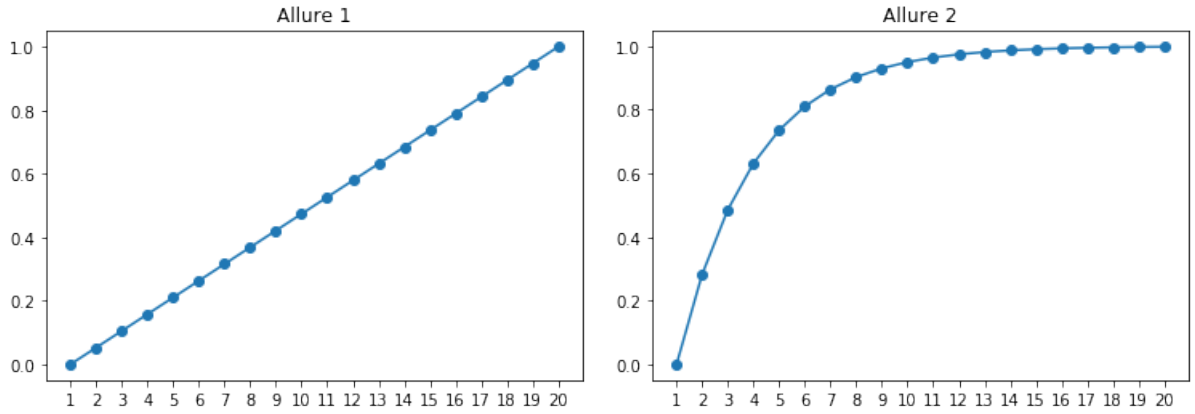

Figure 7: Coordinates of two examples of kernels for the mean shift $\mathbf{u}$ ($r_a = 0$)

This allows us to estimate, using $N = 10^6$ simulations, the probability of conflict for different values of d, which we group together in this table:

Distance	Probability	Error (95%)
1	0.53	±0.00099
2	0.24	±0.00086
3	0.068	±0.0005
4	0.011	±0.0002136
5	0.0011	±6.6E-05
6	6.35E-05	±2.6E-06
7	2.37E-06	±1.0E-07
8	4.33E-08	±6.1E-09
9	4.93E-10	±8.1E-11
10	4.60E-12	±1.0E-12
11	1.55E-14	±3.9E-15
12	3.96E-17	±8.9E-18
13	5.50E-20	±1.4E-20

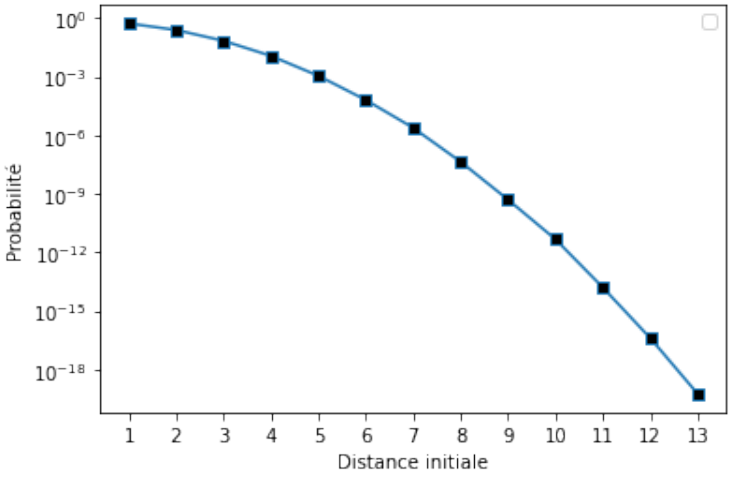

Figure 8: Conflict probability, parallel trajectories, $r_a = 0$

When $r_a \neq 0$:

When $r_a \neq 0$, we simulate, in addition to the distribution of the abscissas of the airplanes, that of the ordinates, we must adapt for this purpose the definition of collision to involve the two vectors, but the change of mean remains similar and deals only with *cross-track* coordinates. In this case, we observe good performance of the estimator for the following shape of **u**:

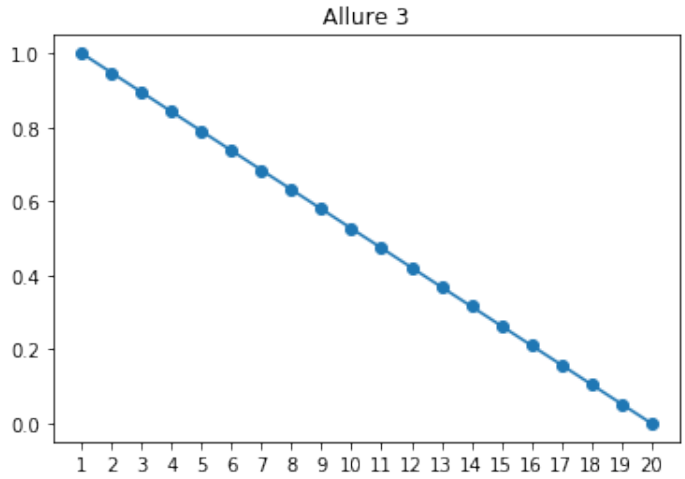

Figure 9: Choix de **u** ($r_a = 0.25$)

The conflict probabilities ($N = 10^6$) :

Distance	Probability	Error(95%)
1	0.027	±0.00033
2	0.0076	±0.00017
3	0.0015	±7.8E-05
4	0.000221	±3.0E-05
5	1.37E-05	±3.1E-06
6	7.73E-07	±2.0E-07
7	2.05E-08	±5.5E-09
8	2.51E-10	±1.2E-10
9	2.59E-12	±2.9E-13
10	1.21E-14	±2.1E-15

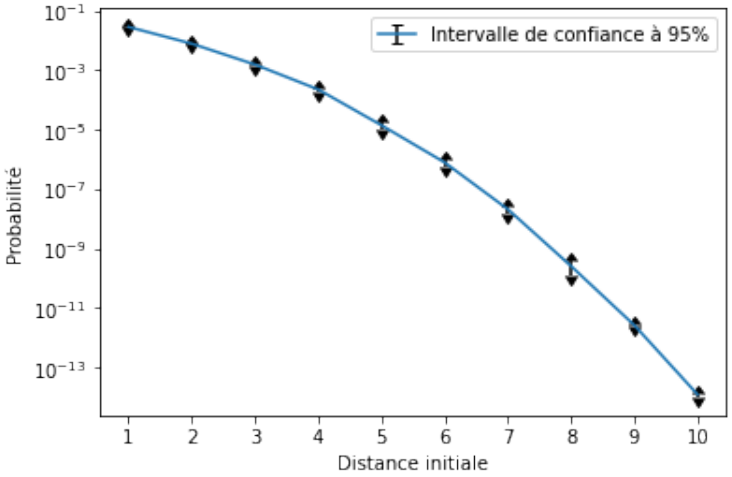

Figure 10: Probabilités de conflit, trajectoires parallèles, $r_a = 0.25$

Interprétation :

When $r_a = 0$, we obtain better results for more pronounced changes in mean towards the end of the trajectory, and we have the opposite for $r_a = 0.25$. We have noticed that the correct choice of the **u** pace depends on the conditional distribution of the conflict time, which we will see more closely in a later part.

3.3.4 • Markov Chains Monte Carlo Methods :

A stationary AR(1) process is defined by induction as follows (for simplicity, we place ourselves in dimension 1). We fix $\rho \in]-1, 1[$, we choose $X_{k0} \sim \mathcal{N}(2\mu_k, 2\mathbb{C}\text{ov}_k)$ and we set, for $i \geq 1$ and $k \in \{a, c\}$ with a representing the along-track component and c representing the across-track component.

$$X_{ki}^A := \begin{cases} \rho(X_{k(i-1)}^A - 2\mu_k) + \sqrt{1-\rho^2}(Y_{ki} - 2\mu_k) + 2\mu_k & \text{if in } A \\ X_{k(i-1)}^A & \text{if not} \end{cases} \tag{1}$$

Where $(Y_{ki})_{i\geq 1}$ is a sequence of i.i.d. random variables of distribution $\mathcal{N}(2\mu_k, 2\mathbb{C}\text{ov}_k)$, independent of X_{k0} which represents the difference between two parralel trajectories and A being a measurable set over which we condition. It is therefore a process which is renewed between two instants by keeping part of the old trajectory $(\rho X_{k(i-1)})$ and adding a part of innovation $(\sqrt{1-\rho^2}Y_{ki})$.

1. for all $i \geq 0$, X_{ki}^A is a gaussian vector with mean $2\mu_k$ and covariance matrix $2\mathbb{C}\text{ov}_k$ conditioned to belong to A,

2. the ergodic theorem remains valid: for any measurable subset B of R^{20}

$$\frac{1}{n}\sum_{i=1}^{n} 1_{X_{ki}^{A}\in B} \quad \underset{n\to\infty}{\longrightarrow} \quad \mathbb{P}(Z \in B \,|\, Z \in A) \tag{2}$$

and where $Z \sim \mathcal{N}(2\mu_k, 2\mathbb{C}\text{ov}_k)$.

So the idea here is to find:

$$threshold = a_0 < a_1 < \cdots < a_m = initial\ distance \tag{3}$$

And then estimate each of the conditional probabilities $\mathbb{P}(Z > a_\ell \,|\, Z > a_{\ell-1})$ via a method still based on (2), using $n = 2.10^3$ and $\rho = 0.85$.

Finally, to calculate $\mathbb{P}(Z \in A)$, we use the formula

$$\mathbb{P}(Z \in A) = \prod_{\ell=1}^{k} \mathbb{P}(Z \in A_\ell \,|\, Z \in A_{\ell-1}) \tag{4}$$

where each conditional probability is approximated via (2).
The probabilities obtained when $r_a \neq 0$ are given in the following table:

Distance	Probability	Error (95%)
1	0.027	±0.00035
2	0.0081	±0.00018
3	0.000931	±2.9E-05
4	0.00022	±6.6E-06
5	1.36E-05	±5.0E-07
6	7.08E-07	±3.0E-08
7	4.48E-08	±1.7E-09
8	5.43E-10	±4.9E-11
9	3.95E-12	±3.9E-13
10	1.61E-14	±2.9E-15
11	1.37E-16	±2.0E-17
12	1.17E-18	±5.0E-19
12.2	4.47E-20	±5.2E-21

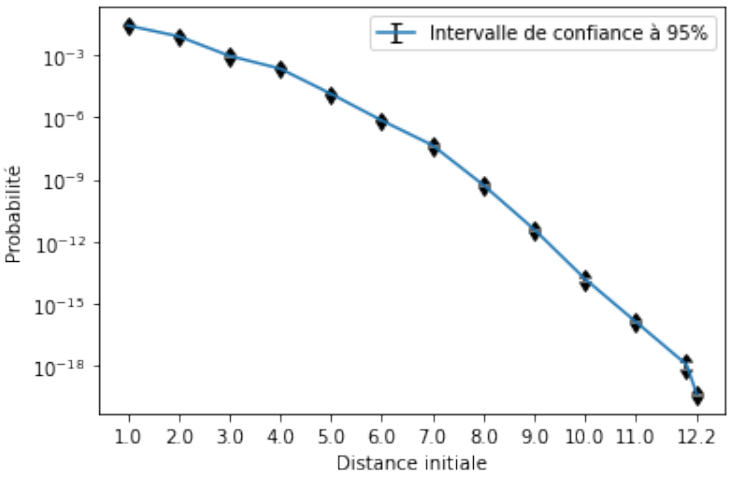

Figure 11: Conflict probability, parralel trajectories, $r_a = 0.25$

The MCMC algorithm returns values in agreement with those calculated previously and allows us to go further in the estimation of low probabilities of conflict.

4
CONFLICT PROBABILITY : CROSSING TRAJECTORIES

4.1 Perpendicular trajectories

We now consider two perpendicular flight planes, intersecting near the middle, but not quite, so as to introduce an offset of the horizontal trajectory which provides for a minimum distance d between the two planes.

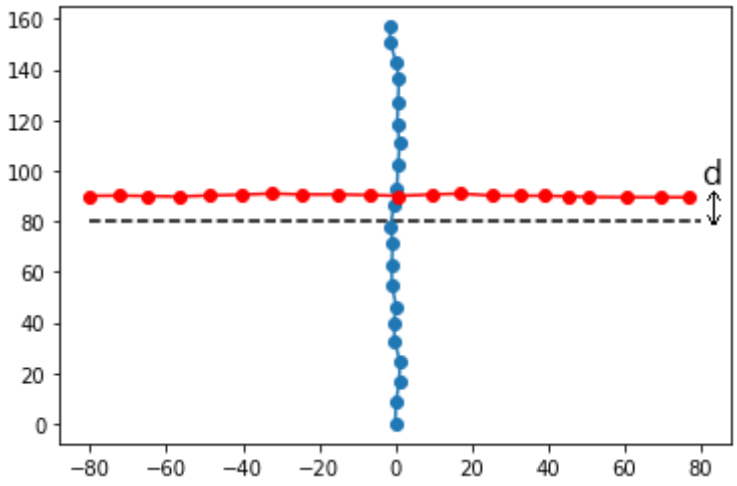

Figure 12: Illustration of the case studied

We now seek to calculate, as a function of the distance d, for $r_a = 0$, the probability of conflict.

4.1.1 • Without *along-track* uncertainty

Once again, the *cross-track* coordinates of the two planes are obtained by generating standard Gaussian vectors, on which we perform a mean change similar to the parallel case, before transforming the coordinates to bring back the planes of flights in the perpendicular case.

Here we expect the collision to take place somewhere in the middle of the trajectories, which is why we use the following kernels for the mean change:

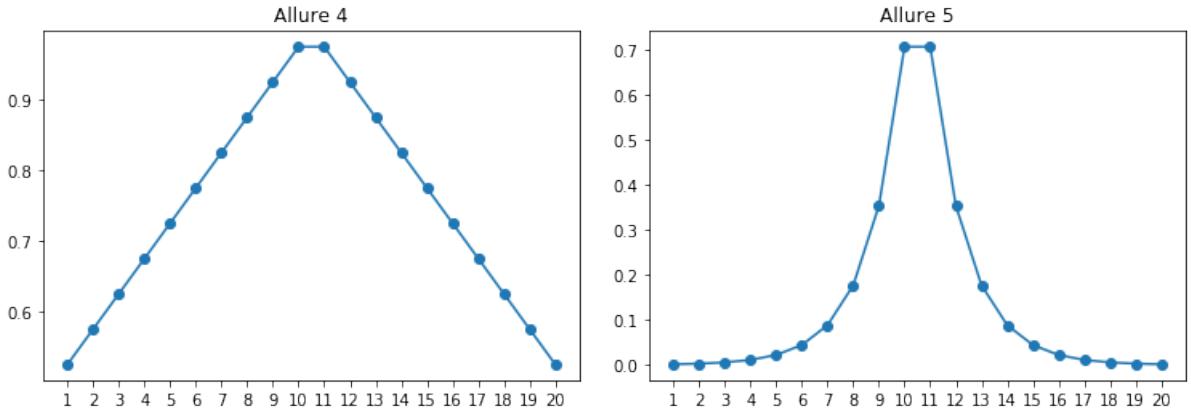

Figure 13: Two choices of kernels $\mathbf{u}$ with point effect

We obtain the following values ($N = 10^6$):

Distance	Probability	Error(95%)
1	0.003105	±0.00011
2	0.000649	±5.1E-05
3	4.5E-05	±1.3E-05
4	1.02E-06	±3.2E-07
5	2.23E-09	±7.2E-10
6	1.29E-11	±3.8E-12

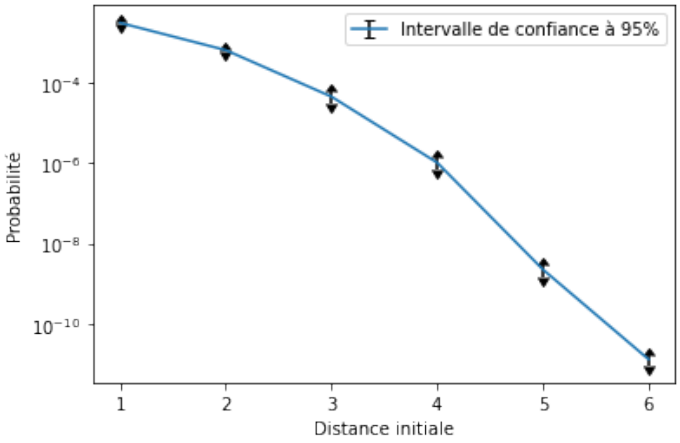

Figure 14: Conflict probabilities, perpendicular trajectories, $r_a = 0$

When $r_a = 0.25$, the mean shift becomes much less efficient. Indeed, the cumulative uncertainty on the *along-track* coordinate makes the local approximation between nominal trajectories ineffective when it comes to producing collisions. This therefore calls for another type of importance sampling, for example based on a change in variance of the *along-track* uncertainty.

4.2 Inclined trajectories

We go back to the case $r_a = 0$, in a more general context, we consider trajectories intersecting near the middle, forming a non-particular angle (for example $\frac{\pi}{4}$) and we We also introduce a

minimum separation distance d, to observe the effect of the latter on the probability of conflict, a similar importance sampling method gives the following results ($N = 10^6$):

Distance	Probability	Error(95%)
1	0.00155	±7.9E-05
2	1.5E-05	±7.8E-06
2.5	2.15E-07	±9.0E-08
3	1.1E-09	±8.0E-10

4.3 About MCMC

The disadvantage of the methods used until now lies in the fact that our algorithms must be calibrated according to the chosen flight plan, and do not easily adapt to different cases. The aim of using the MCMC method was to overcome this problem and develop a more generic method. But we could not observe satisfactory results as to its performance for the case of inclined trajectories, although it (MCMC) was shown to be superior for parallel trajectories. Indeed, the implementation turned out to be more delicate, in particular in terms of the calculation of the various quantiles.

5 CONDITIONAL DISTRIBUTION

5.1 Distribution of the time of conflict

In this part, we try to determine the distribution, conditional on the occurrence of the conflict, of the time of the latter and this for several distances d. For that, we place ourselves again in the case of parallel trajectories. Let $\{T = k\}$ be the event "The collision takes place at the k-th minute", we therefore seek to estimate $\mathbb{P}(T = k|T \leq 20)$, for this we calculate a confidence interval for the probability $\mathbb{P}(T = k)$, and using the conflict probabilities and errors calculated previously, we can calculate an interval for the ratio

$$\frac{\mathbb{P}(T = k)}{\mathbb{P}(T \leq 20)} = \mathbb{P}(T = k|T \leq 20)$$

Analogously to the case of crossed trajectories, we adopt a "local" change of mean so as to favor the conflicts at the instant k, we therefore use shapes of the type (4) and (5), by adjusting the peak at the time concerned.

5.1.1 • When $r_a = 0$

For small distances, the distribution can be calculated precisely using Monte Carlo simulations, and looks like this for different values of d:

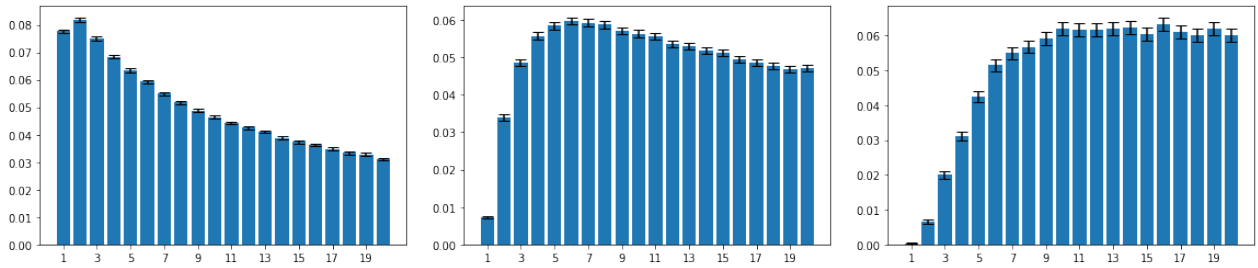

Figure 15: Conditional distribution of the time of conflict, from left to right : $d = 1$, $d = 2$, $d = 3$

For greater distances, estimation using importance sampling gives the following appearance:

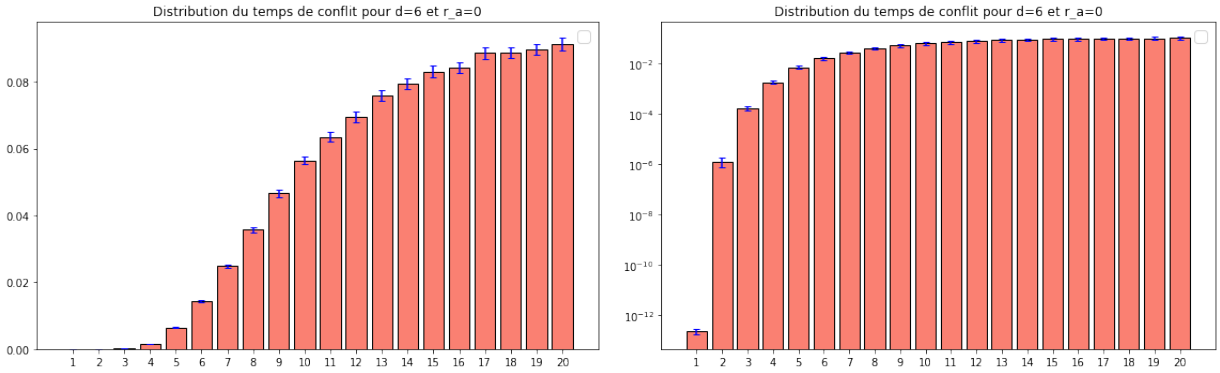

Figure 16: Conditional distribution of the time of conflict for $d = 6$ in normal and logarithmic scales

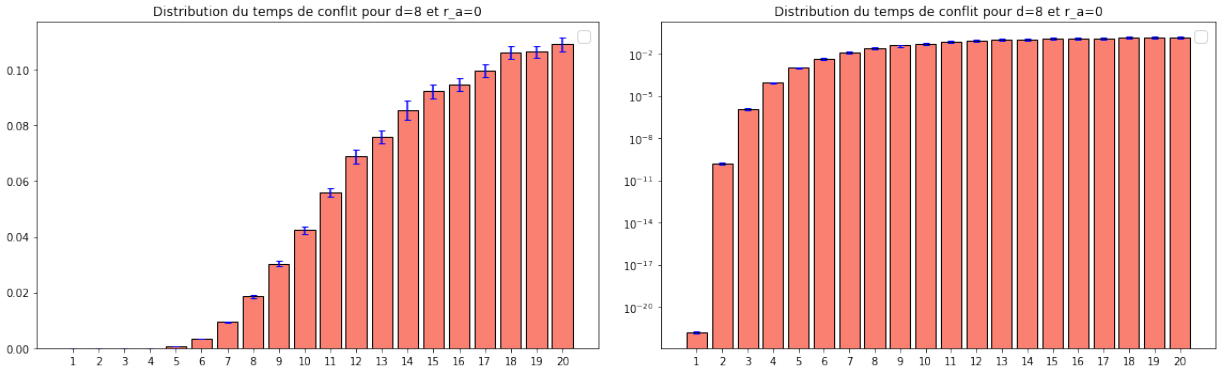

Figure 17: Conditional distribution of the time of conflict for $d = 8$ in normal and logarithmic scales

5.1.2 • When $r_a \neq 0$

For small distances, the distribution can be calculated precisely using Monte Carlo simulations, and looks like this for different values of d:

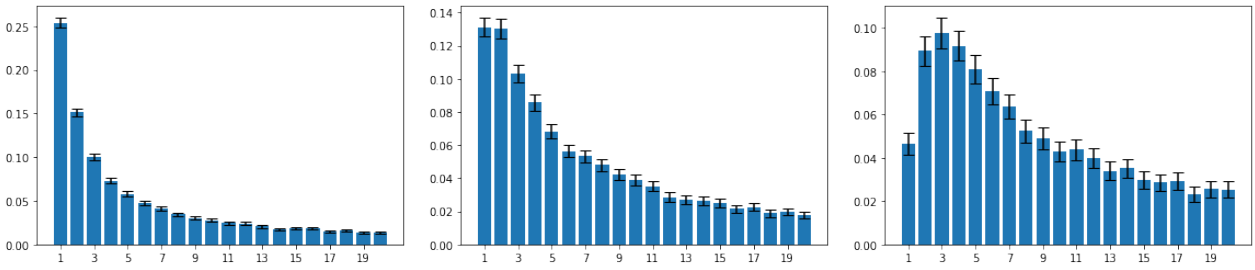

Figure 18: Conditional distribution of the time of conflict, from left to right : $d = 1$, $d = 1.5$, $d = 2$

For greater distances, the estimate using large-scale sampling gives the following appearance:

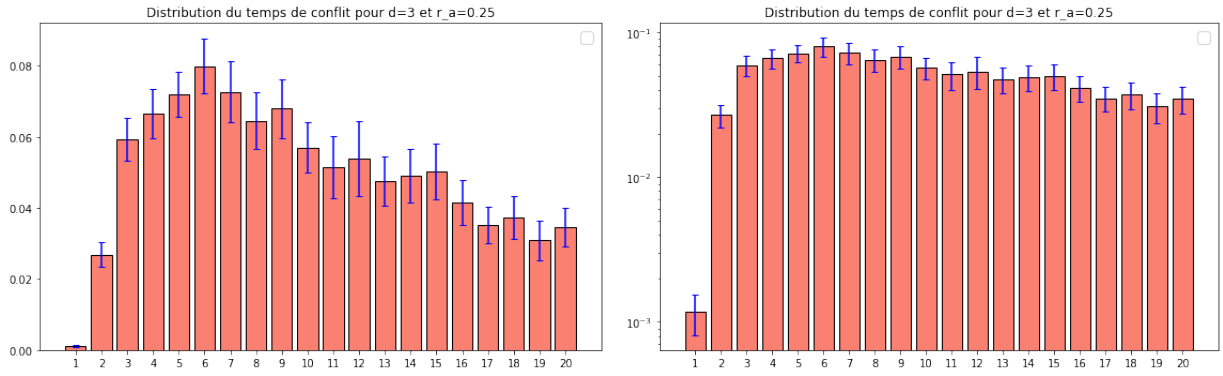

Figure 19: Conditional distribution of the time of conflict for $d = 3$ in normal and logarithmic scales

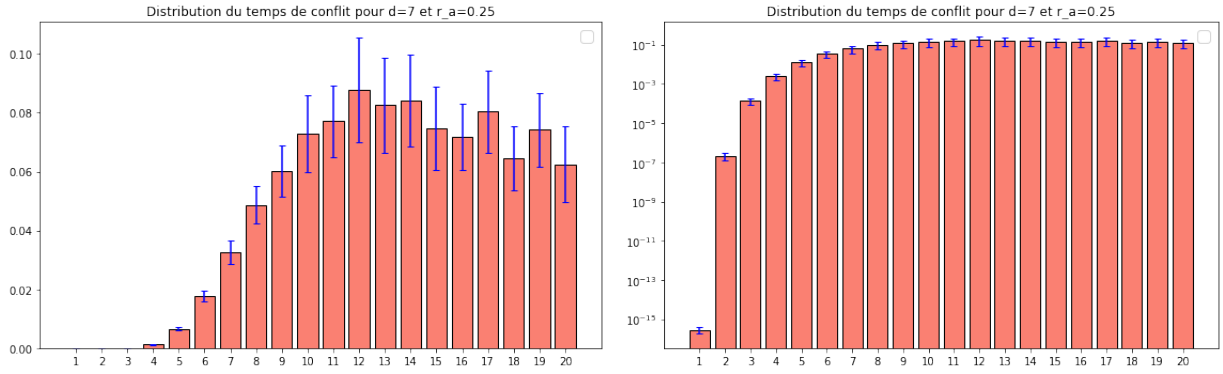

Figure 20: Conditional distribution of the time of conflict for $d = 7$ in normal and logarithmic scales

For $r_a = 0.25$, we have a phenomenon similar to the case $r_a = 0$, but the increasing uncertainty on the *along-track* component means that the conditional probability is not maximal towards the end but shortly before, and this maximum translates as the initial distance between the planes increases.

5.2 Distribution of the conflict position

We are now interested in the distribution, conditional on the occurrence of the conflict, of the position of the latter. For that, we plot, for different values of the distance d, and for a very large number of simulations ($N = 10^7$), the 2D histogram of the collisions in the case of parallel trajectories.

5.2.1 • $r_a = 0$

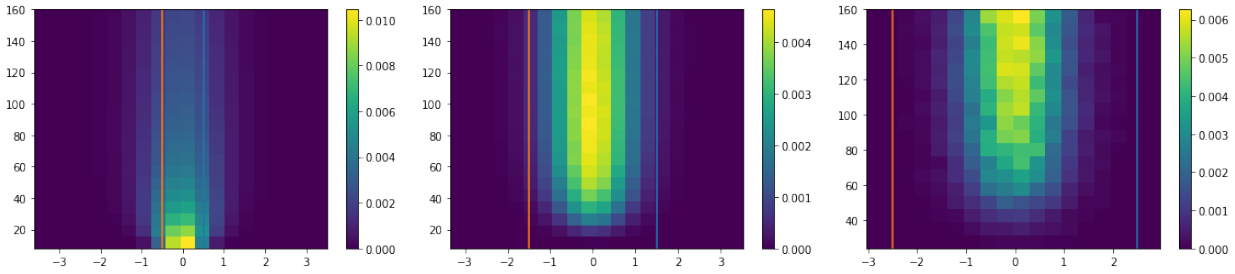

Figure 21: Conditional distribution of the position of conflict, from left to right : $d = 1$, $d = 3$, $d = 5$ ($r_a = 0$), the lines represent the nominal trajectories of the planes.

As one might expect, this distribution approximates the conflict time distribution. As the distance increases, the collisions are localized more and more towards the end of the trajectory, they are also more and more confined between the trajectories.

5.2.2 • $r_a \neq 0$

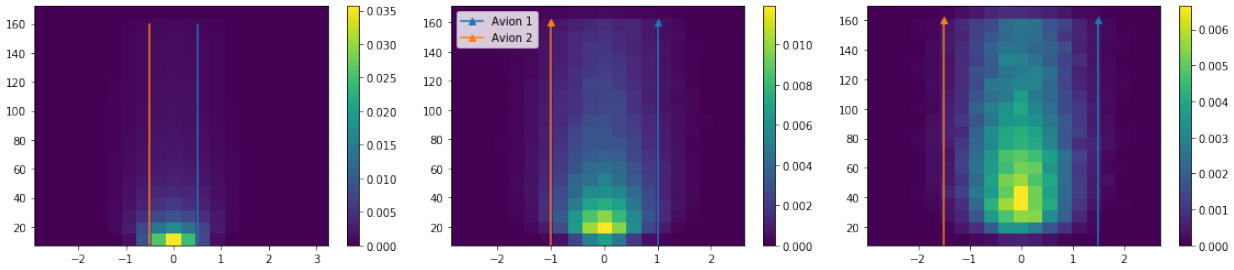

Figure 22: Conditional distribution of the position of conflict, from left to right : $d = 1$, $d = 2$, $d = 3$ ($r_a = 0.25$), the lines represent the nominal trajectories of the planes.

Again, the distribution is characterized by a maximum because of the *along-track* uncertainty.

6 CONCLUSION

The order of magnitude of the probabilities of the events studied means that their statistical analysis becomes very delicate and requires an adapted approach. During this study, we managed to approach very low probabilities for relatively simple cases and others more general, based on important sampling methods adapted to the characteristics of the model, and we could notice the considerable increase in precision obtained by the right choice of probability changes. But the methods used must be calibrated according to the flight plans considered. We tried to adopt an MCMC algorithm to overcome this problem, but did not reach satisfactory results for the case of inclined trajectories. Finally, we used the tools at our disposal to examine the distribution in time and space of conflicts between airplanes, and were able to confirm our intuitions about the model, and to better understand its behavior and the influence of this on the airplanes.

REFERENCES

[1] Maria Prandini; Oliver J. Watkins : Probabilistic aircraft conflict detection. 30 May 2005.

[2] Heinz Erzberger Russel A.Paielli : Conflict probability estimation for free flight. *NASA Ames Research Center.*

[3] Edward Nelson : Dynamical theories of brownian motion. *Department of Mathematics, Princeton University.*

[4] Jianghai Hu; Maria Prandini et Shankar Sastry : Aircraft conflict prediction in the presence of a spatially correlated wind field.

[5] Benjamin Jourdain et Jérôme Lelong : Robust adaptive importance sampling for normal random vectors.